Application of Neutron Activation Techniques for the Measurement of ^{238}U (n, γ) and ^{238}U (n, 2n) Cross Section at Neutron Energies of 13.5 and 17.28 MeV

Sadhana Mukerji[*1], H. Naik[2], S. V. Surayanarayana[3], B.S. Shivashankar[4], V. K. Mulik[5], Sachin Chachara[1], Sudipta Samanta[1], A.Goswami[2], P.D.Krishnani[1]

[1]Reactor Physics Design Division, Bhabha Atomic Research Centre, Mumbai-400 085, India
[2]Radiochemistry Division, Bhabha Atomic Research Centre, Mumbai -400 085, India
[3]Nuclear Physics Division, Bhabha Atomic Research Centre, Mumbai -400 085, India
[4]Department of Statistics, Manipal University, Manipal - 576 104, India
[5]Department of Physics, University of Pune, Pune - 411 007, India
[*1]mukerjis@barc.gov.in

***Abstract*-The (n, γ) and (n, 2n) reaction cross-section of ^{238}U at average neutron energies of 13.5 and 17.28 MeV from the ^{7}Li(p, n)^{7}Be reaction has been determined using activation and off-line γ–ray spectrometric technique. The experimentally determined ^{238}U(n, γ)^{239}U and ^{238}U(n, 2n)^{237}U reaction cross-sections from present work were compared with the evaluated data of ENDF/BVII.0 and JENDL-4.0, JEFF-3.1/A and CENDL-3.1 (referenced in text). The experimental values were found to be in general agreement with the evaluated values obtained using ENDF/BVII.0, JENDL-4.0 and JEFF-3.1/A but it differs with the values obtained using CENDL-3.1. The present data along with literature data in a wide range of neutron energies were interpreted in terms of competition between ^{238}U(n, γ), (n, f), (n, nf) and (n, xn) reactions channels. The ^{238}U(n, γ) and ^{238}U(n, 2n) reaction cross-sections were also calculated theoretically using the TALYS 1.4 computer code and were found to be in general agreement with the experimental data.**

Keywords- ^{238}U (n, γ)^{239}U and ^{238}U(n, 2n)^{237}U Reaction Cross-Sections; ^{7}Li(p, n)^{7}Be Reaction; Average Neutron Energy; E_n = 13.5 and 17.28 MeV; Off-Line γ-Ray Spectrometric Technique; TALYS Calculation

I. INTRODUCTION

One of the major components of the nuclear waste comprises of long-lived minor actinides such as ^{237}Np, ^{240}Pu, ^{241}Am, ^{243}Am and ^{244}Cm. Almost all the minor actinides are generated due to capture (n, γ) and (n, 2n) reactions of ^{238}U and ^{239}Pu followed by beta decay. For electricity generation, for many decades, Light Water Reactors (both pressurised and boiling type PWR & BWR) or Heavy Water Reactors (HWR) is primary reactors of choice. In these reactors appreciable amount of ^{237}Np is produced by (n, 2n) and (n, γ) reactions. The fuels used in these reactors are mainly based on enriched or natural uranium. ^{237}Np is one of the most problematic minor actinides generated in these reactors. After million of years, ^{237}Np dominates in terms of radio-toxicity to the population because of the leakage of the actinide from the disposal site. In order to avoid this, the concept of advanced heavy water reactor AHWR [1, 2] has been proposed in the recent past to generate nuclear power. In AHWR, ^{232}Th-^{233}U in the oxide form is used as the primary fuel, where the production of long lived minor actinides such as ^{237}Np, ^{237}Np, ^{240}Pu, ^{241}Am, ^{243}Am and ^{244}Cm can be avoided. Significant effort has also been made to developed fast reactor [3-7] to fulfil the increased demand of power production. In the fast reactor ^{238}U-^{239}Pu in the form of carbide is used as the primary fuel. Since the fast reactor has a fast neutron spectrum, the production of long-lived minor actinides can be suppressed. The ^{239}Pu used in the fast reactor is first generated in a research reactor from ^{238}U(n, γ)^{239}U reaction followed by successive two beta decays. A schematic diagram of (n, γ) and (n, 2n) reaction of ^{238}U followed beta decay in the U-Pu fuel cycle is shown below.

$$\begin{array}{ccccccc} & & & \beta^- & & \beta^- & \\ ^{238}\text{U}\,(n,\gamma) & \rightarrow & ^{239}\text{U} & \rightarrow & ^{239}\text{Np} & \rightarrow & ^{239}\text{Pu} \\ 4.468\times10^{19}\text{ y} & & 23.45\text{ m} & & 2.357\text{ d} & & 24110\text{ y} \\ \downarrow (n,2n) & & & \beta^- & & \beta^- & \downarrow (n,2n) \\ ^{237}\text{U} & \rightarrow & ^{237}\text{Np}\,(n,\gamma) & \rightarrow & ^{238}\text{Np} & \rightarrow & ^{238}\text{Pu} \\ 6.75\text{ d} & & 2.144\times10^{6}\text{ y} & & 2.117\text{ d} & & 87.7\text{ y} \end{array}$$

DOI: 10.5963/JBAP0202009

In the fast reactor, ^{238}U is used as the breeding material to regenerate the fissile material ^{239}Pu. Thus the production of fissile nucleus ^{239}Pu depends on the ^{238}U(n, γ)^{239}U reaction cross-section, which is required with an accuracy of 1-2% for predicting the dynamical behaviour of complex arrangements in fast reactors [8, 9] safely. In fusion-fission hybrid systems, a sensitivity study has shown that the production rate of ^{239}Pu can be predicted within 1%, provided that the ^{238}U(n, γ)^{239}U cross-section between 3 keV and 3 MeV is known within 2 % [10]. In fast breeder reactors the most important region for neutron capture of ^{238}U lies between 10 keV and 100 keV [11]. At neutron energy of 100 keV, the ^{238}U(n, γ)^{239}U reaction cross-section shows a sharp increase trend due to resonance neutron capture. Thereafter it decreases up to 6-7 MeV, where the ^{238}U(n, 2n)^{237}U reaction cross-section starts. The fast reactor has harder neutron spectrum with neutron energy up to 15 MeV, whereas the ^{238}U(n, 2n)^{237}U reaction cross-section has threshold energy of 6.18 MeV. Thus above the neutron energy of 6.18 MeV, the ^{238}U(n, 2n)^{237}U reaction is one of the reaction channels besides (n, f) and (n, γ) reactions of ^{238}U. Above neutron energy of 6.18 MeV, the ^{238}U(n, 2n)^{237}U reaction cross-section increases rapidly. Thus the ^{238}U(n, γ)^{239}U and ^{238}U(n, 2n)^{237}U reactions cross-sections at higher neutron energy have a strong impact on the performance and safety assessment for fast reactor [12].

Besides the above two reactions, ^{239}Pu(n, γ)^{240}Pu and ^{239}Pu(n, 2n)^{238}Pu reactions will also occur in the fast reactor. Out of these two reactions, ^{239}Pu(n, 2n)^{238}Pu is of interest from its application point of view. ^{238}Pu is used as a heat source in radio thermal generators to produce electricity for a variety of purposes including unmanned spacecraft and interplanetary probe. ^{238}Pu is also generated through ^{237}Np(n, γ)^{238}Np reaction followed by successive beta decay. However, ^{237}Np itself is generated from ^{238}U(n, 2n)^{237}U reaction followed by beta decay. Thus at various neutron energies, it is necessary to have knowledge about the ^{238}U(n, 2n)^{237}U reaction cross-section besides the ^{238}U(n, γ)^{239}U reaction cross-section.

The ^{238}U(n, γ)^{239}U reaction cross-section data are available in the literature over a wide range of neutron energies from thermal to 18 MeV based on physical measurements [13-23] and activation technique [24-33]. Similarly, sufficient data on ^{238}U(n, 2n)^{237}U reaction cross-section are also available in a wide range of neutron energy above 6 MeV from off-line γ-ray spectrometry and neutron activation methods [33-39].

From the literature data [13-33], it can be seen that the ^{238}U(n, γ)^{239}U reaction has numerous resonance cross-section from thermal energy to 0.1 MeV. However, above neutron energy of 0.1 MeV the ^{238}U(n, γ)^{239}U reaction cross-section decreases up to 6-7 MeV [24, 26-28]. Above neutron energy of 7 MeV, the ^{238}U(n, γ)^{239}U reaction cross-section data of D. K. Mc Daniels et al. [22] decrease sharply and remain almost constant up to14 MeV. At neutron energy of 9.85 MeV, the data of H. Naik et al. [33] are comparable to the data of D. K. Daniels et al. [22]. At neutron energy of 17 MeV, the ^{238}U(n, γ)^{239}U reaction cross-section data of Yu. G. Panitkin et al. [26, 27] and V. A. Tolstikov et al. [28] increase sharply and thereafter remain constant up to 20 MeV. Within neutron energy of 6.18-20 MeV, the ^{238}U(n, 2n)^{237}U reaction becomes the pre-dominant mode besides (n, γ) and (n, f) reaction of ^{238}U. It can be seen from Refs. [33-39] that the increase of ^{238}U(n, 2n)^{237}U reaction cross-section is very sharp from the neutron energy of 6.18 MeV to 7-8 MeV and then remains constant up to 13-14 MeV. Thereafter, it decreases with increase of neutron energy due to opening of other channels such as (n, 2nf) and (n, xn) reactions.

II. DESCRIPTION OF THE EXPERIMENT

The 14UD BARC-TIFR Pelletron facility at Mumbai, India [33] was used to carry out the present experiment. The proton beam main line at 6 m height above the analysing magnet of the Pelletron facility was utilize to obtained the neutron beam by using the ^{7}Li(p, n)^{7}Be reaction. The proton energies of the experiment were 16 and 20 MeV, respectively. The energy spread for proton beam was maximum 50-90 keV. A collimator of 6 mm diameter was used before the Li target to avoid the energy spread of the proton beam. The lithium foil used for neutron production was made up of natural lithium with thickness of 3.7 mg/cm^2, sandwiched between two tantalum foils of different thickness. The front tantalum foil facing the proton beam has a thickness of 3.9 mg/cm^2, in which degradation of proton energy is only 30 keV. On the other hand the back tantalum foil has a thickness of 0.025 mm, which is sufficient to stop the proton beam. Behind the Ta-Li-Ta stack, the samples used for irradiation were placed.

The samples consist of natural ^{238}U metal foil, wrapped with 0.025 mm thick super pure aluminium foil of purity 99.999%. The aluminium wrapper was used as a catcher to stop fission products recoiling out from the ^{238}U metal foil during irradiation. The size of ^{238}U metal foil was 1.0 cm^2 with thickness of 29.3 mg/cm^2. The U sample wrapped with Al was mounted at zero degree with respect to the beam direction at a distance of 2.1 cm from the location of the Ta-Li-Ta stack. A schematic diagram of Ta-Li-Ta stack and sample is given in Fig. 1. Different sets of Ta-Li-Ta stacks and U sample wrapped with Al were made for different irradiations at various neutron energies.

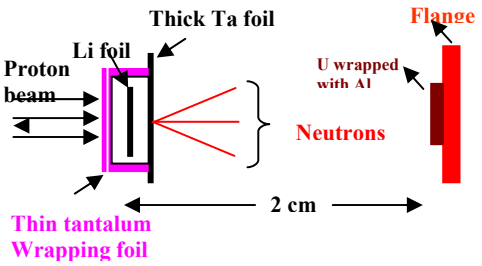

Fig. 1 Schematic diagram showing the arrangement used for neutron irradiation

DOI: 10.5963/JBAP0202009

The U sample along with Al wrapper was irradiated by the neutrons generated by impinging the proton beam on the lithium metal foil through the thin tantalum foil of the Ta-Li-Ta metal stack. In the first set, the irradiation time was 7 h for neutron beam corresponding to the proton beam energy of 16 MeV. Similarly, in the second set, the irradiation time was 6 h for neutron beam corresponding to the proton beam energy of 20 MeV. The proton current during the irradiations varied from 300-400 nA. For the proton energies of 16 and 20 MeV, the corresponding maximum neutron energies faced by U samples targets were 13.5 and 17.28 MeV, respectively. After irradiation, the samples were cooled for sufficient time (6-24 h). Then the irradiated target of U along with Al wrapper were mounted on different Perspex plates and taken for γ-ray spectrometry.

The γ-rays of fission/reaction products from the irradiated U sample was done at BARC using pre-calibrated HPGe detector connected to a PC based 16K GAMMA FAST MCA with High Voltage Power Supply Card. The detector is a coaxial p-type HPGe detector from EURASIS, France with relative efficiency of 50%. The resolution of the detector system was 2 keV at 1332.5 keV of ^{60}Co. The detector has a 3'' lead shielding on all sides to reduce the background of the system. The measurements were repeated for several times to follow the decay of the radio nuclides. Measurements were done at suitable distance between the sample and the end cap of the detector to keep the dead time within 5% to avoid pileup effects. The γ-ray counting of the sample was done in live time mode and was followed as a function of time. The energy and efficiency calibration of the detector system was done by counting the γ-ray energies of standard ^{152}Eu and ^{133}Ba sources [40-42] keeping the same geometry, where the summation error was negligible. The uncertainty in the efficiency was 2-3%. The γ-ray counting of the irradiated U samples were done up to few months to check the half-life of the nuclides of interest. A typical γ- ray spectrum from the irradiated ^{238}U sample for ^{238}U(n, γ)^{239}U and ^{238}U(n, 2n)^{237}U reactions are given in Fig. 2.

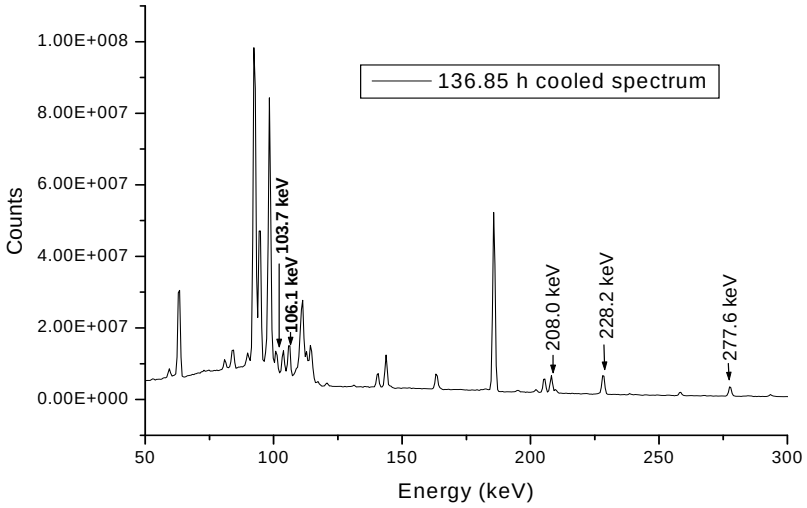

Fig. 2 Gamma ray spectrum of irradiated ^{238}U showing the γ-ray energy of ^{237}U and ^{239}Np

III. ANALYSIS OF THE EXPERIMENT

A. Calculation of the Neutron Energy

In the present experiment, the incident proton energies used were 16 and 20 MeV, respectively. Neutrons are generated by the ^{7}Li(p, n)^{7}Be reaction. However, different reaction takes place when the proton beam heats the natural lithium target. Natural lithium consists of isotopes ^{6}Li and ^{7}Li with abundances 7.42% and 92.58% respectively. The degradation of the proton energy on the front thin tantalum foil of 4 mg/cm^2 thickness is only 30 keV. The Q-value for the ^{7}Li(p, n)^{7}Be reaction to the ground state is -1.644 MeV, where as for the first excited state is 0.431 MeV above the ground state leading to an average Q-value of -2.075 MeV. The ground state of ^{7}Be is having the threshold of 1.881 MeV, whereas the first excited state of ^{7}Be is having the threshold of 2.38 MeV. With ^{7}Li, a second neutron group at $E_P \geq 2.4$ MeV is produced due to the population of the first excited state of ^{7}Be. Thus for the proton energy of 16 and 20 MeV, the corresponding first group of (n_0) neutron energies are 14.12 and 18.12 MeV to the ground state of ^{7}Be. For the first excited state of ^{7}Be, the neutron energy of the second group of neutrons (n_1) will be 13.62 and 17.62 MeV, respectively. Fragmentation of ^{8}Be* to ^{4}He+^{3}He+n (Q= -3.23 MeV) also occurs when the proton energy exceeds the value 4.5 MeV and the other reaction channels are open to give continuous neutron distribution besides n_0 and n_1 groups of neutrons. The branching ratio to the ground and first excited state of ^{7}Be up to proton energy of 7 MeV is given in the Refs. [43, 44], where as for proton energies from 4.2 MeV to 26 MeV is given in the Ref. [45]. For the proton energies of 16 and 20 MeV, the neutron spectra are continues one besides n_0 and n_1 group of neutrons. To observe the trend of continuous neutron spectrum, we have generated (Fig. 3) it by using the neutron energy distribution given in Refs. [43-45]. This distribution is obtained by shifting the peak by -0.5 MeV. So for the proton energies of 16 and 20 MeV the peak of the neutron energies distribution are around 14.12 and 18.12 MeV (this scaling has been done due to the fact that

DOI: 10.5963/JBAP0202009

the maximum neutron energy from ^{7}Li(p, n) reaction cannot exceed (E_P -1.88) MeV. After removing the tailing distribution, the average neutron energies under the main peak region were obtained as 13.50 ± 0.35 and 18.28 ± 0.35 MeV for the proton energy of 16 and 20 MeV, respectively.

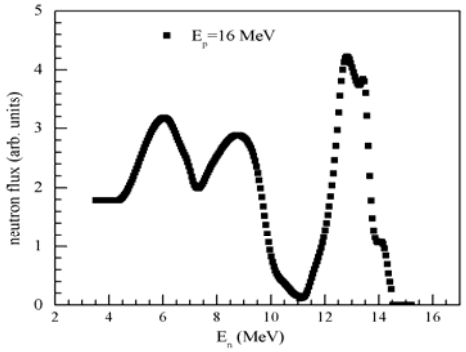

Fig. 3 Neutron spectrum from ^{7}Li(p, n) reaction at E_p=16.0 MeV calculated using the results of Meadows and Smith of Ref. [44]

B. Calculation of the Neutron Flux

The neutron flux was calculated using the yield (Y) of fission products such as ^{97}Zr, extracted from the experimental yields of Refs. [46, 47] assuming that the yields of asymmetric fission products in the fast neutron induced fission of ^{238}U do not change significantly with neutron energy. The equation used for such calculation is as follows.

$$\Phi = \frac{A_{net}\,(CL/CT)\lambda}{N\langle\sigma\rangle Ya\varepsilon(1-e-\lambda t)(e-\lambda t)(1-e-\lambda CL)} \tag{1}$$

where A_{net} is the net area of the full energy photo-peak, which was calculated using the PHAST peak fitting program [48]. N is the number of target atoms and σ_f is the ^{238}U(n, f) cross-section taken from ref. [49]. 'a' is the branching intensity of the gamma lines used and ε is its detection efficiency. 't', T , CL and LT are the irradiation time, cooling time, clock time and counting time respectively. In the above equation the CL/LT term has been used for dead time correction. At average neutron energy of 13.5 and 17.28 MeV, the neutron flux calculated using Eq. (1) are (7.87± 0.12) x10^6 n cm^{-2} s^{-1} and (9.16±0.17) x10^7 n cm^{-2} s^{-1}, respectively. Folding the neutron spectrum of Fig. 3 and Fig. 4 [45] with ^{238}U(n, f) cross section [49] at different neutron energies gives average fission cross-section.

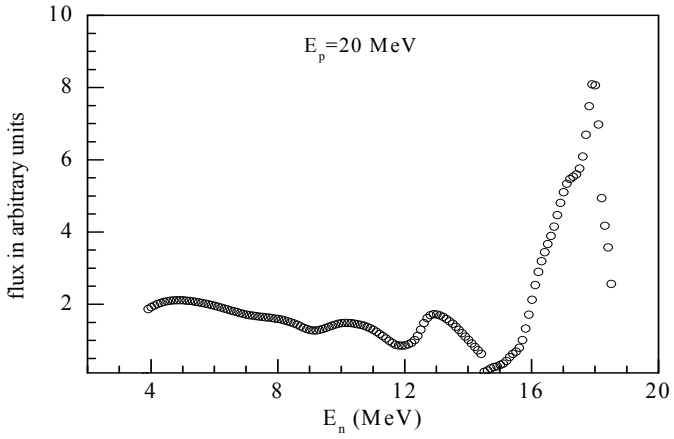

Fig. 4 Neutron spectrum from ^{7}Li(p, n) reaction at E_p=20.0 MeV calculated using the results of Meadows and Smith of Ref. [44]

C. Determination of ^{238}U(n, γ)^{239}U and ^{238}U(n, 2n)^{237}U Reaction Cross-Sections and Their Results

For the calculation of ^{238}U(n, γ)^{239}U and ^{238}U(n, 2n)^{237}U reactions cross-sections, the nuclear spectroscopic data used in the present work, are taken from the Refs. [40-42] and are given in Table 1. It can be seen from Table 1 that the reaction product ^{239}U has the half-life of 23.54 min. Within 3 h, it decays 99.6% to its daughter product ^{239}Np having half-life of 2.355 days. In the present experiment, since the cooling time of the irradiated samples were 6-24 h, more than 99.6% of ^{239}U has decays to its daughter product ^{239}Np. Thus the ^{238}U(n, γ)^{239}U reaction cross-section (σ) can be calculated from the γ-ray activity of ^{239}Np

DOI: 10.5963/JBAP0202009

measured after sufficient cooling time (6-24 h). For the calculation of the $^{238}U(n, 2n)^{237}U$ reaction cross-section, the γ-ray activity of ^{237}U was used after 24-48 hours. The net area of the full energy photo-peak (A_{net}) for the γ-lines of ^{237}U and ^{239}Np are obtained by using PHAST [48] fitting program. The net photo-peak (A_{net}) for the γ-lines of ^{237}U and ^{239}Np is related to the cross-sections (σ) for the $^{238}U(n, \gamma)^{239}U$ and $^{238}U(n, 2n)^{237}U$ reactions with the Eq. (2) as

$$\sigma = \frac{A_{net}(CL/LT)\lambda}{N\phi a\varepsilon(1-e^{-\lambda t})(e^{-\lambda t})(1-e^{-\lambda CL})} \quad (2)$$

All terms in Eq. (2) have the similar meaning as in the Eq. (1).

TABLE I NUCLEAR SPECTROSCOPIC DATA USED IN THE CALCULATION TAKEN FROM REFS. [40-42]

S. No	Nuclide	Half life	γ-ray energy (keV)	γ-ray abundance (%)
1	U-237	6.75 d	101.1	26.0
			208.0	22.0
2	U-239	23.54 m	74.7	52.2
3	Np-239	2.355d	103.7	23.9
			106.1	22.7
			228.2	10.7
			277.9	14.2
4	Zr-97	16.9 h	743.3	92.8

At average neutron energy of 13.5 MeV, the neutron flux (Φ) of (7.87±0.12) x10^6 and (6.69±0.14) x10^6 n cm^{-2} s^{-1} were used in Eq. (2) to calculate the $^{238}U(n, \gamma)^{239}U$ and $^{238}U(n, 2n)^{237}U$ reaction cross-sections, which are 1.992±0.08 and 1516.75±105.98 mb, respectively. Similarly, at average neutron energy of 17.28 MeV the neutron flux (Φ) of (9.16±0.17) x10^7 and (6.96±0.18) x10^7 n cm^{-2} s^{-1} were used to calculate the $^{238}U(n, \gamma)^{239}U$ and $^{238}U(n, 2n)^{237}U$ reaction cross-sections, which are 1.276±0.07 mb and 1001.58±25.6 mb, respectively.

It can be seen from Fig. 3 and Fig. 4 that there is substantial contribution to the neutron flux from the tail region at the proton energy of 16 and 20 MeV, respectively. Thus for $^{238}U(n, \gamma)^{239}U$ reaction, the low energy neutrons also contribute to the cross-section. In view of this the contribution from the tail region to $^{238}U(n, \gamma)^{239}U$ reaction has been estimated using the evaluated nuclear data file ENDF/B-VII [50] and Japanese evaluated nuclear data library JENDL-4.0 [51] by folding the cross-sections with neutron flux distributions. The contribution to the cross-section of the $^{238}U(n, \gamma)^{239}U$ reaction from the above evaluation at E_P = 16 MeV are 1.325 mb and 0.972 mb from ENDF/B-VII [50] and JENDL-4.0 [51], respectively. Similarly, at E_P = 20 MeV, the contribution to the cross-section of the $^{238}U(n, \gamma)^{239}U$ reaction from the above evaluation are 0.86 mb and 0.612 mb from ENDF/B-VII [50] and JENDL-4.0 [51], respectively. The actual value of $^{238}U(n, \gamma)^{239}U$ reaction-cross section due to the neutrons from the main peak of the n_0 and n_1 groups of the neutron spectrum is obtained after subtracting the average cross-section due to neutrons from tail region from the before mentioned experimental data. Thus the actual experimentally obtained $^{238}U(n, \gamma)^{239}U$ reaction cross-sections at average neutron energies of 13.5 and 17.28 MeV corresponding to proton energy of 16 MeV and 20 MeV are 0.844±0.08 mb and 0.546±0.07 mb, which are given in Table 2. In a similar way, the contribution to the $^{238}U(n, 2n)^{237}U$ reaction cross-section due to the tailing part of the neutron spectrum was evaluated. These are about 497.2 mb from ENDF/B-VII.0 [50] and 493.5 mb from JENDL-4.0 [51] for the average neutron energies of 13.5 corresponding to proton energy of 16 MeV. Similarly, at average neutron energy of 17.28 MeV corresponding to proton energy of 20 MeV, these are 558.43 mb from ENDF/B-VII.0 [50] and 531.2 mb from JENDL-4.0 [51], respectively. Thus the actual experimentally obtained $^{238}U(n, 2n)^{237}U$ reaction cross-section at average neutron energy of 13.5 and 17.28 MeV from present work are 1021.37± 106.0 mb and 456.78 ±25.6 mb, which are given in Table 2.

TABLE II $^{238}U(N, \Gamma)^{239}U$ AND $^{238}U(N, 2N)^{237}U$ REACTION CROSS-SECTIONS AT DIFFERENT NEUTRON ENERGIES

Neutron Energy (MeV)	Neutron Flux (n/cm^2 /sec)	Cross Section (mb)		
		Expt.	ENDF/B-VII.0	JENDL-4.0
$^{238}U(n, \gamma)^{239}U$				
13.5	(7.87±0.12) x 10^6	0.844± 0.080	0.930	0.656
17.28	(9.16±0.17) x 10^7	0.546± 0.070	0.460	0.277
$^{238}U (n, 2n)^{237}U$				
13.5	(6.69±0.14) x 10^6	1021.37±106.00	1049.4	1294.8
17.28	(6.96±0.18) x 10^7	456.78± 25.60	331.43	327.9

For $^{238}U(n, \gamma)^{239}U$ and $^{238}U(n, 2n)^{237}U$ reactions the neutron energies are 13.5 and 17.28 MeV.

DOI: 10.5963/JBAP0202009

The uncertainties associated to the measured cross-sections come from the combination of two experimental data sets. This overall uncertainty is the quadratic sum of both random and systematic errors. The random error in the observed activity is primarily due to counting statistics of γ-ray activities of reaction products ^{239}Np from ^{238}U(n, γ) reaction and ^{237}U from ^{238}U(n, 2n) reaction, which is estimated to be 10-15%. This can be determined by accumulating the data for an optimum time period that depends on the half-life of nuclides of interest. The systematic errors are due to uncertainties in neutron flux estimation (~4%), correction in the ^{238}U(n, γ)^{239}U and ^{238}U(n, 2n)^{237}U reaction cross-sections due to the tail part of the neutron (~4%) the irradiation time (~2%), the detection efficiency calibration (~3%), the half-life of the reaction/fission products and the γ-ray abundances (~2%) as reported in references [40-42]. Thus the total systematic error is about 7%. The overall uncertainty is found to range between 12 to 17%, coming from the square root of quadratic sum of a statistical error of 10-15% and a systematic error of 7%.

IV. DISCUSSION

The ^{238}U(n, γ)^{239}U and ^{238}U(n, 2n)^{237}U reaction cross-sections at average neutron energies of 13.5 and 17.28 MeV of present work are determined using a neutron source from ^{7}Li(p, n) reaction. Since the average neutron energies of 13.5 and 17.28 MeV were obtained from ^{7}Li(p, n) reaction at proton energies of 16 and 20 MeV, the neutron spectrum has some tailing (Fig. 3 and Fig. 4). Thus the correction to the ^{238}U(n, γ)^{239}U and ^{238}U(n, 2n)^{237}U reaction cross-section due to the tail part of the neutron spectrum have been taken care, which has been mentioned in the analysis section. Same approach has been used in the earlier work [33] for the measurement of neutron induced reaction cross-section of ^{238}U at neutron energies of 3.7 and 9.85 MeV corresponding to the proton energies of 5.6 and 12 MeV, respectively. In order to examine the validity of the present approach, the experimentally determined ^{238}U(n, γ)^{239}U and the ^{238}U(n, 2n)^{237}U reaction cross-sections were compared with the evaluated data from ENDF/B-VII.0 [50], JENDL 4.0 [51], Joint evaluation fission and fusion nuclear data library JEFF-3.1/A [52] and Chinese evaluated nuclear data library CENDL-3.1 [53]. These evaluated reaction cross-sections for ^{238}U(n, γ)^{239}U reaction from ENDF/B-VII.0 [50] and JENDL 4.0 [51] are quoted in Table 2 for the neutron energies of 13.5 and 17.28 MeV because of the finite width of neutron energy under the main peak of Fig. 3 and Fig 4. Similarly for the ^{238}U(n, 2n)^{237}U reaction, the evaluated cross-sections from ENDF/B-VII.0 [50] and JENDL 4.0 [51] in Table 2 are quoted for the neutron energies of 13.5 to 17.28 MeV. It can be seen from the Table 2 that the present experimental ^{238}U(n, γ)^{239}U and ^{238}U(n, 2n)^{237}U reaction cross-sections are within the range of evaluated data of ENDF/B-VII.0 [50] and JENDL 4.0 [51], showing consistency with our present approach and experimental results. The evaluated data from JEFF-3.1/A [52] are same as of ENDF/B-VII.0 [50] and thus not shown in Table 2. However, the evaluated data from CENDL-3 [53] are not in agreement with the present experimental values and thus are not quoted in Table 2. In Fig. 5, we present a detailed study comparing our results with various evaluations and available experimental data of the ^{238}U(n, γ)^{239}U reaction cross-sections, and also discuss inconsistencies of the available data from literature [13-33] given in EXFOR [54] in various neutron energy regions.

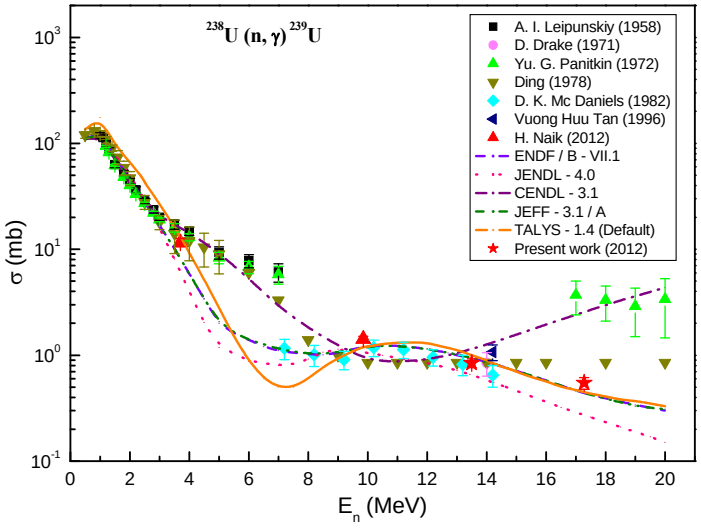

Fig. 5 Plot of experimental and evaluated ^{238}U(n, γ)^{239}U reaction cross-section as a function of neutron energy from 1 keV to 20 MeV. Experimental values from present work and from Refs. [13-33] are in different symbols, whereas the evaluated and theoretical values from TALYS are in solid line of different colour

From Fig. 5, it can be seen that the ^{238}U(n, γ)^{239}U reaction cross-section from present work at 13.5 MeV is in agreement with the value of Mc Daniels et al [22]. However, the ^{238}U(n, γ)^{239}U reaction cross-section from present work at 17.28 MeV is lower than the value of Patikin et al [27]. Besides this, it can be seen from Fig. 5 that the ^{238}U(n, γ)^{239}U reaction cross-section

DOI: 10.5963/JBAP0202009

decreases systematically from 100 keV to 7 MeV. However, at neutron energy of 7 MeV, the data of Mc Daniels et al [22] are suddenly lower compared to the data of Leipunskiy et al [24] and Patikin et al [26]. From the neutron energy of 7 to 15 MeV, the data of Mc Daniels et al [22] remain almost same. Beyond neutron energy of 17 MeV, the experimental data obtained by Patikin et al [27] suddenly increase and then remain almost constant up to 20 MeV. For a comparison, the data of Ding et al. [56] based on neutron activation technique from the review article were shown in Fig. 5. Further the evaluated $^{238}U(n, \gamma)^{239}U$ reaction cross-section data from ENDF/B-VII.0 [50], JENDL-4.0 [51], JEFF-3.1/A [52], CENDL [53] and INDC (VN)-8 [55] were also shown in Fig. 5. From Fig. 5, it can be seen that the evaluated data of CENDL [53] are in agreement with the earlier data from references [13-32]. However, the evaluated data of CENDL [53] disagree with the present data and other evaluations. The trend of evaluated data from CENDL [53] is entirely different than the evaluated data from ENDF/B-VII.0 [50], JENDL-4.0 [51] and JEF-3.1/A [52]. Further, the data of Ding et al [56] show agreement with the present experimental data and evaluated data from ENDF/B-VII.0 [50], JENDL-4.0 [51] and JEF-3.1/A at lower energy only and significantly differ at higher energy. The experimental data of present work at 13.5 and 17.28 MeV as well as the data of Mc Daniels et al [22] at 7-15 MeV are in good agreement with the evaluated data of ENDF-B-VII.0 [50], JENDL [51] and JEF-3.1/A [52]. The experimental data of Leipunskiy et al [24] and Patikin et al [26] also show a good agreement with the evaluated data [50-52] within neutron energy of 1-4 MeV. However, the experimental data of Leipunskiy et al [24] and Panitkin et al [26] at neutron energy of 5-7 MeV and of Panitkin et al [27] at 17-20 MeV are higher then the evaluated data [50-52]. To examine this aspect, the $^{238}U(n, \gamma)^{239}U$ reaction cross-section within neutron energy of 1 keV to 20 MeV was also calculated theoretically using computer code TALYS of version 1.4 [57] as done earlier [33] and are shown in the Fig. 5.

From Fig. 5, it can be seen that the $^{238}U(n, \gamma)^{239}U$ reaction cross-section [50-54] obtained using TALYS 1.4 computer code [57] reproduces the trend of evaluated data of ENDF/B-VII.0 [50], JENDL-4.0 [51] and JEF-3.1/A. However, within neutron energy of 1 keV to 3 MeV, the theoretical $^{238}U(n, \gamma)^{239}U$ reaction cross-section from TALYS are slightly higher than the experimental and evaluated values. This may be due to the use of default parameters in TALYS. However, the values from TALYS are in close agreement with the value of our present work at 13.5 and 17.28 MeV as well as with the values of Mc Daniels et al [22] at 7-14 MeV. On the other hand, the experimental values of Leipunskiy et al [24] and Panitkin et al [26] at neutron energy of 5-7 MeV and of Panitkin et al [27] at 17-20 MeV are higher than the theoretical value of TALYS code [57]. Higher experimental value at 5-7 MeV by Leipunskiy et al [24] and Panitkin et al [26] could be due to the contribution from the low energy scattered neutrons of the D+D neutron source. Similarly, the higher experimental value at 17-20 MeV by Panitkin et al [27] may be due to the contribution from the low energy scattered neutron of the D+T neutron source. As also mentioned by Panitkin et al [27], at low energy scatted neutrons contribute to the higher $^{238}U(n, \gamma)^{239}U$ reaction cross-section. Therefore, subtracting out the contribution (n, γ) cross section from low energy tailing neutrons is important to compare with Talys calculations and other evaluations. In the present work we also found higher uncorrected cross-sections (Table 2) due to lower energy tail part in the neutron spectrum from $^{7}Li(p, n)$ reaction. Thus the contribution to the $^{238}U(n, \gamma)^{239}U$ reaction cross-section due to the low energy tail part of neutrons has been estimated and subtracted out, which has been mentioned earlier in our calculation. As mentioned before, our experimental data agree well with evaluations and TALYS results.

Besides the above observations, the experimental [13-33], evaluated [50-53] and the theoretical [57] $^{238}U(n, \gamma)^{239}U$ reaction cross-section decreases from 100 keV to 7 MeV and predict a dip in around 6-8 MeV as shown in Fig. 5. The dip in the $^{238}U(n, \gamma)^{239}U$ reaction cross-section around neutron energy of 6-8 MeV indicates the opening of (n, 2n) reaction channel besides (n, nf) channel. Above 8 MeV, it increases and shows a bump up to the neutron energy of 14 MeV and then again decreases. This can be understood from the saturated $^{238}U(n, 2n)^{237}U$ reaction cross-section above 8 MeV. In order to illustrate this, $^{238}U(n, 2n)^{237}U$ reaction cross-section from the present work and references [33-39] given in EXFOR [54] along with the evaluated data [50, 51] were shown in Fig 6. The $^{238}U(n, 2n)^{237}U$ reaction cross-sections at different neutron energy was also calculated theoretically using computer code TALYS of version 1.4 [57] and plotted in Fig. 6. From Fig. 6, it can be seen that the $^{238}U(n, 2n)^{237}U$ reaction cross-section from TALYS shows a close agreement with the experimental data within neutron energy of 8 MeV. Above 8 MeV, the TALYS results seem to over predict the experimental data. Further it can be seen from Fig. 6 that the experimental and theoretical $^{238}U(n, 2n)^{237}U$ reaction cross-sections show a sharp increasing trend from the neutron energy of 6.18 MeV to 8 MeV and thereafter remains constant up to 14 MeV. Thus the increasing trend of $^{238}U(n, \gamma)^{239}U$ reaction cross-section beyond 8 MeV up to14 MeV in Fig. 5 is due to near constant $^{238}U(n, 2n)^{237}U$ reaction cross-section observed in Fig. 6. It can be also observed from Fig. 5 and Fig. 6 that the $^{238}U(n, \gamma)^{239}U$ reaction cross-section shows a dip, where the $^{238}U(n, 2n)^{237}U$ and $^{238}U(n, nf)$ reaction cross-sections show a sharp increasing trend. Similar trend of (n, γ) and (n, 2n) reactions was seen in case of ^{232}Th within neutron energy of 14 MeV, which is most probably due to sharing of excitation energy between two different reaction channels besides (n, f) reaction channel. Similarly, above neutron energy of 14 MeV due to the opening of (n, 3n) and (n, 2nf) reaction channels, both $^{238}U(n, \gamma)^{239}U$ (Fig. 5) and $^{238}U(n, 2n)^{237}U$ (Fig. 6) reaction cross-sections show a decreasing trend.

DOI: 10.5963/JBAP0202009

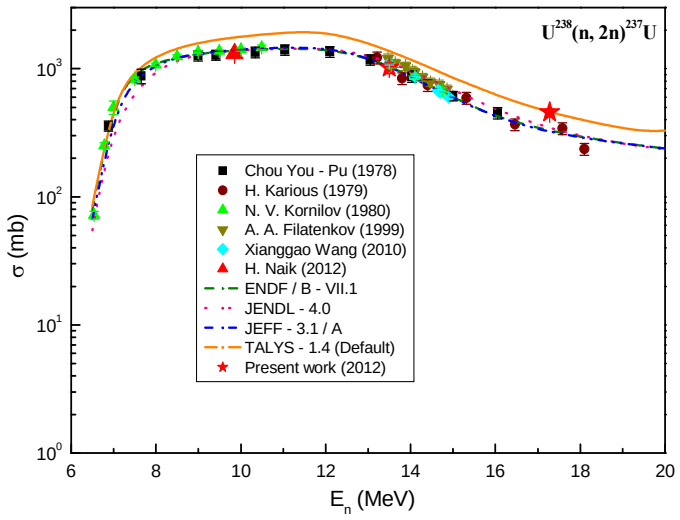

Fig. 6 Plot of experimental and evaluated $^{238}U(n, 2n)^{237}U$ reaction cross-section as a function of neutron energy from neutron energy 5 MeV to 25 MeV. Experimental values from present work and from Refs. [33-38] are in different symbols, whereas the evaluated and theoretical values from TALYS are in solid lines with different colours

V. CONCLUSIONS

(i) The $^{238}U(n, \gamma)^{239}U$ and $^{238}U(n, 2n)^{237}U$ reaction cross-section at average neutron energies of 13.5 and 17.28 MeV are determined using a neutron source from $^{7}Li(p, n)$ reaction. Since the neutrons are not mono-energetic, corrections in the cross sections are incorporated.

(ii) The $^{238}U(n, \gamma)^{239}U$ and $^{238}U(n, 2n)^{237}U$ reaction cross-section at average neutron energy 13.5 and 17.28 MeV are in good agreement with the experimental data from literature and the evaluated data from ENDF/B-VII.0, JENDL-4.0 and JEFF-3.1/A but not with evaluated data from CENDL-3.

(iii) The $^{238}U(n, \gamma)^{239}U$ reaction cross-section decreases from neutron energy of 100 keV to 14 MeV with a dip at 6-8 MeV. The $^{238}U(n, 2n)^{237}U$ reaction increases sharply in the energy range from 6.18 MeV to 8.0 MeV and thereafter it remains constant up to the neutron energy of 14 MeV. Beyond neutron energy of 14 MeV both $^{238}U(n, \gamma)^{239}U$ and $^{238}U(n, 2n)^{237}U$ reaction cross-sections show decreasing trend due to opening of (n, 3n) and (n, 2nf) reaction channels.

(iv) The $^{238}U(n, \gamma)^{239}U$ and $^{238}U(n, 2n)^{237}U$ reaction cross-sections were calculated theoretically using TALYS code version 1.4. The TALYS results for $^{238}U(n, \gamma)^{239}U$ reaction cross-section over predict the experimental data within the neutron energy of 1 keV to 3 MeV and thereafter it is agreement with the experimental data. However, the TALYS results for $^{238}U(n, 2n)^{237}U$ reaction cross-sections are in good agreement with the experimental data up to 8 MeV and thereafter over predict the experimental data.

ACKNOWLEDGMENT

The authors are thankful to the staff of TIFR-BARC Pelletron facility for their kind co-operation and help to provide the proton beam to carry out the experiment. We are also thankful to Mr. Ajit Mahadkar and Mrs. Dipa Thapa from target laboratory of Pelletron facility at TIFR, Mumbai for providing us the Li and Ta targets.

REFERENCES

[1] R.K. Sinha and A. Kakodkar "Design and Development of AHWR– The Indian Thorium Fueled Innovative reactor," Nucl. Eng. Des., 236, 7-8 (2006) 683.

[2] S. Ganesan, "Creation of Indian Experimental Benchmarks for Thorium Fuel Cycle," IAEA Coordinated research project on "Evaluated Data for Thorium- Uranium fuel Cycle," Third Research Co-ordination Meeting, 30 January to 2 February 2006, Vienna, Austria, INDC (NDS) - 0494 (2006).

[3] Fast Reactors and Accelerator Driven Systems Knowledge Base, IAEA-TECDOC- 1319: Thorium fuel utilization: Options and Trends.

[4] P. E. MacDonald and N. Todreas, Annual Project Status Report 2000, MIT-ANP-PR-071, INEFL/EXT-2009-00994.

[5] L. Mathieu et al., "Proportion for a very simple Thorium Molten Salt reactor," Proc. Global International Conference, Paper No. 428,

DOI: 10.5963/JBAP0202009

Tsukuba, Japan, 2005.

[6] A.Nuttin, D. Heuer, A. Billebaud, R. Brissot, C. Le Brun, E. Liatard,J. M. Loiseaux, L. Mathieu, O. Meplan, E. Merle-Lucotte, H. Nifenecker, F. Perdu and S. David, Proc. Nucl. Energy 46 (2005) 77.

[7] T.R. Allen and D.C. Crawford, Science and Technology of Nuclear Installations, Article ID 97486 (2007).

[8] V. G. Pronyaev, "Summary Report of the Consultants' Meeting on Assessment of Nuclear Data Needs for Thorium and Other Advanced Cycles," INDC (NDS) - 408, International Atomic Energy Agency (1999).

[9] B. D. Kuz'minov and V. N. Manokhin, "Status of Nuclear Data for Thorium Fuel Cycle," Nucl. Constants, 3-4 (1997) 41.

[10] E. T. Cheng and D. R. Mathews, "The Influence of Nuclear Data Uncertainties on Thorium Fusion-Fission Hybrid Blanket Nucleonic Performance," Proc. Int. Conf. Nuclear Cross Sections for Technology, Knoxville, Tennessee, October 22-26, 1979 p. 834, NBS-SP 594, National Bureau of Standards.

[11] D. E. Bartine, "The Use of Thorium in Fast Breeder Reactors," Proc. Int. Conf. Nuclear Cross Sections for Technology, Knoxville, Tennessee, October 22-26, 1979, p. 119, NBS-SP 594, National Bureau of Standards.

[12] S. Pelloni, G. Youinou and P. Wydler, "Impact of Different Nuclear data on the performance of fast spectrum based on the Thorium-Uranium fuel cycle," Proc. Int. Conf. Nuclear data for Science and Technology, Trieste, Italy, May 19-24, 1997, Part II, p.1172.

[13] R. Batchelor, W.B. Gilboy, J.H. Jowle, Nucl. Phys. 65 (1965) 236.

[14] M. Asghar, C.M. Chaffey, M.C. Moxon, Nucl. Phys. 85 (1966) 305.

[15] H.O. Menlok and W.P. Poenitz, Nucl. Sci. Eng. 33 (1968) 24.

[16] D. Drake, I. Bergqvist and D.K. McDaniels, Phys. Lett. B 36 (1971) 557-559.

[17] G.D. Saussure, E.G. Silver, R.B. Perez, R. Ingle, H. Weaver, Nucl. Sci. Eng. 51 (1973) 385.

[18] W. P. Poenitz, Nucl. Sci. Eng. 57 (1975) 300.

[19] H.L. Liou and R.E. Chrien, Nucl. Sci. Eng. 62 (1977) 463.

[20] K. Wisshak and F. Kappeler, Nucl. Sci. Eng. 66 (1978) 363.

[21] R.B. Perez, G. de. Saussure, R.L. Macklin, J. Halperin, Phys. Rev. C 20 (1979) 528.

[22] D. K. Mc Daniels, P. Varghese, D.M. Drake, F. Arthur, A. Lindholm, I. Berquist, J. Krumlinde, Nucl. Phys. A 384 (1982) 88.

[23] J. Voignier, S. Joly, G. Grenier, Nucl. Sci. Eng. 112 (1992) 87.

[24] A. I. Leipunskiy, O. D. Kazachkovskiy, G. Ja. Artyukhov, A. I. Baryshnikov, T. S Belanova, V. I. Galkov, Yu. Ja. Stavisskiy, E. A. Stumbur, L. E. Sherman, 58GENEVA, 15 (1958) 50.

[25] R.C. Hann and B. Rose, J. Nucl. Eng. 8 (1959) 197.

[26] Yu. G. Panitkin and V. A. Tolstikov, Atomnaya Energia, 33 (1972) 782.

[27] Yu. G. Panitkin and V. A. Tolstikov, Atomnaya Energia, 33 (1972) 825.

[28] Yu. G. Panitkin and V. A. Tolstikov, Atomnaya Energia, 39 (1975) 17.

[29] M. Lindner, R.J. Nagle, J.H. Landrum, Nucl. Sci. Eng. 59 (1976) 381.

[30] W.P. Poenitz, L.R. Fawcell Jr., D.L. Smith, Nucl. Sci. Eng. 78 (1981) 329.

[31] N.N. Buleeva, A.N. Davletshin, O.A.Tipunkov, S.V. Tikhonov, V.A. Tolstokov, Atomnaya Energia, 65 (1988) 348.

[32] E. Quang and G.F. Knoll, Nucl. Sci. Eng. 110 (1991) 282.

[33] H. Naik, S.V. Suryanarayana, V.K. Mulik, P.M. Prajapati, V.S. Shivashankar, K.C. Jagadeesan, S.V. Thakare, D. Raj, S.C. Sharma, P.V. Bhagwat, S.D. Dhole, S. Ganesan, V.N. Bhoraskar, A. Goswami, J. Radianal. Nucl. Chem. 293 (2012) 469.

[34] J.H. Landrum, R.J. Nagle, M. Lindner, Phys. Rev. C 8 (1973) 1938.

[35] H. Kaius, A. Ackermann, W. Scobel, J. Phys. G. 5 (1979) 715.

[36] J. Frchaut, A. Bertin, R. Bois, Nucl. Sci. Eng. 74 (1980) 29.

[37] N. V. Kornilov, B. V. Zhuravlev, O. A. Sal'nikov, P. Raich, Sh. Nad', Sh. Darotsi, K. Sailer and I. Chikai , Atomnaya Energia, 49 (1980) 283.

[38] G. Shani, Ann. Nucl. Energy, 10 (1983) 473.

[39] X. Wang, S. Jiang, M. He, K. Dong, C. Xiao, Nucl. Ins. Meth. in Physics Research A 621 (2010) 326.

[40] E. Browne and R.B. Firestone, Table of Radioactive Isotopes, ed. V.S. Shirley (1986); E. Browne, Nuclear Data Sheets 93 (2001) 763; R.B. Firestone, L.P. Ekstrom, Table of Radioactive Isotopes, (2004).

[41] J. Blachot and Ch. Fiche, Table of Radioactive Isotopes and their main decay characteristics, Ann. de Phys. 6 (1981) 3-218; J. Blachot, Nuclear Data Sheets, 104 (2005) 967-1110.

[42] B. Singh, J. K. Tuli, Nuclear Data Sheets 105 (2005) 109-222.

[43] H. Liskien and A. Paulsen, "Neutron Production Cross Sections and Energies for the Reactions 7Li(p,n)7Be and 7Li(p,n)7Be*," At. Data Nucl. Data Tables, 15 (1975) 57.

[44] J.W. Meadows, D.L. Smith, Neutrons from proton bombardment of natural lithium, Argonne National Laboratory Report ANL-7983 (1972).

[45] C. H. Poppe, J. D. Anderson, J.C. Davis, S.M. Grimes, and C. Wong Phys. Rev. C 14 (1976) 438.

[46] S. Nagy, K.F. Flynn, J.E. Gindler, J.W. Meadows, L.E. Glendenin, Phys. Rev. C 17 (1978) 163.

[47] T.C. Chapman, G.A. Anzelon, G.C. Spitale, D.R. Nethaway, Phys. Rev. C 17 (1978) 1089.

[48] P. K. Mukhopadhyaya, Personal Communication (2001).

DOI: 10.5963/JBAP0202009

[49] J. Blons, C. Mazur, and D. Paya, Phys. Rev. Lett. 35 (1975) 1749.

[50] M.B. Chadwick et al., "ENDF/B-VII.0: Next Generation Evaluated Nuclear Data Library for Nuclear Science and Technology," Nuclear Data Sheets, 107 (2006)2931-3060.

[51] K. Shibata et al., "JENDL – 4.0; A New Library for Nuclear Science and Engineering," J. Nucl. Sci. Tech., 48 (1) (2011) 1.

[52] A. J. Koning, et al., "The JEFF evaluated data project," Proceeding of the International Conference on Nuclear Data for Science and Technology, Nice, 2007.

[53] China Evaluated Nuclear Data Library CENDL-3.1, (2009).

[54] IAEAEXFOR Database, at http://www-nds.iaea.org/exfor.

[55] Vuong Tan, Nguyen Canh Hai, Nguyen Trong Hiep, INDC (VN)-8 (1996).

[56] Ding Da-Zhao, Guo Tai-Chang HSJ-77106, Review of U-238 capture cross-section –En =1 keV to 20 MeV (1978).

[57] A.J. Koning, S. Hilaire and M.C. Duijvestijn, Proceeding of the International Conference on Nuclear Data for Science and Technology-ND 2004, AIP Vol.769, Edited by R.C. Haight, M.B. Chadwick, T. Kawano and P. Talou (Santa Fe, 2005), P. 1154.

DOI: 10.5963/JBAP0202009